# Extraction of Maximum Power of Grid Connected PV System Using Advanced FLC

Md. Naiem-Ur-Rahman*, Dr. Md. Masud Rana**‡, Dr. Md. Fayzur Rahman***

*Department of Electrical and Electronic Engineering, Faculty of Science and Engineering, Lecturer, GUB, Dhaka 1207

** Department of Electrical and Electronic Engineering, Faculty of EEE, Professor, RUET, 6204 Rajshahi

*** Department of Electrical and Electronic Engineering, Faculty of Science and Engineering, Professor, GUB, Dhaka 1207

(naiemur@eee.green.edu.bd, md.masud.rana.ruet@gmail.com, drfayzur@eee.green.edu.bd)

‡Corresponding Author; Md. Naiem-Ur-Rahman, Lecturer, Green University of Bangladesh, 220/D, Begum Rokeya Sarani, Dhaka-1207, Bangladesh. Tel: +8801679773928,

naiemur@eee.green.edu.bd

*Received: 09.08.2021 Accepted:21.09.2021*

**Abstract-** In this paper, an advanced fuzzy controller is proposed for extracting maximum power from the PV panel both in fixed and changing conditions; changing conditions mean altering of temperature and irradiation level. This controller functions of extracting maximum power by finding the optimal point of the corresponding condition of the PV panel; known as maximum power point tracker (MPPT). The proposed controller is compared with some conventional along with some intelligence controllers such as P&O, INC, existing fuzzy and fuzzy optimized by a combination of PSO (particle swarm optimization). In each case it shows better performance in tracking the magnitude of the power from the PV panel which is up to 99%. Then the power is fed to the grid after extracting power from PV panel and when additionally, power is transferred to the grid, some losses occur as approximately 1.5% of the extracted power from the panel. From the investigation, it has been seen that there's no undesired spike while tracking power in case of changing conditions. Tracking time is also the fastest when compared with the controllers which is 0.01 second. As the power is transmitted to the grid, THD analysis is also an important consideration and after analysing it, THD level of the grid voltage shows 0.04% after filtering which is very much satisfactory according to the IEEE standard.

**Keywords** FLC, incremental conductance, maximum power point, optimization, photovoltaic array, voltage source controller.

## 1. Introduction

Demand of the electricity will be increased as the fossil fuels are depleting [1], [2] and supposed to increase up to 30% by 2035. As fossil-fuels are on the verge of extinction, nearly 40% CO2 emissions occur due to combustion of fossil-fuels which is one of the main reasons for increasing global warming. So for the generation of electricity, attention has been given to the renewable energy resources [3] and so in electric power generations, renewable energy sources play a vital role [4]. Among the renewable sources: solar energy, wind energy, geothermal, PV systems are widely used in different power systems but solar energy remains as a good alternative due to being clean and available [5]–[7]. As a result, it has become the most highly promising candidate both in research and development of less costly PV devices. As mentioned earlier, solar power is fastest-growing renewable energy being clean, availability and emits no noise during operation[8], [9], it has wide variety of applications namely power supply for rural areas, battery charging, water pumping, domestic and street lighting, electric vehicles, military and some applications, refrigeration and vaccine storage, power plants etc., all in either stand-alone or grid connected configuration[10]–[13]. The power we get normally from PV cell is very scant in comparison to the maximum capacity and also variable in nature. So, a few years ago scientists started to put their concerns on policies to extract as much as power from the PV cells: generally, PV systems can be categorized into three sections: the standalone systems [14], [15], the grid connected systems [16] and the

hybrid system known as PV systems merging with other energy sources[17], [18]. At first, mechanical systems were initialized by rotating the panel and later a device was designed to get the optimum power by moving the operating voltage and current. In spite of some undesired effects, but to overcome, we can replace a DC-DC converter between the cells and load; furthermore, using a controller to find out the maximum power position for the corresponding condition by varying the duty cycle of the connected converter is known as MPPT. Ultimately now in modern days, a big number of MPPT models and algorithms are available in literature. P&O is one of the conventional methods and widely used because of it's simplicity and easy implementation [19]–[22]. It measures voltage and current, then calculates the power. Next the difference between the two successive power is obtained and finally decides the duty cycle. But the major drawbacks are: fluctuations around the MPP resulting significant loss of energy [23], can't track MPP in case of rapidly changing atmospheric conditions, such as broken clouds. To overcome these problems [24], INC method was introduced which continuously calculates the steps and thus measuring the ratio between instantaneous conductance and INC values of the PV system power. Thus able to track the MPP but requires complex and costly control circuits. Recently a lot of attraction has been gained on the design of a suitable controller for MPPT [25]–[29]. In [30], the P&O method was proposed for the PV-based water pumping system and a comparison has been made between theoretical and practical results. In [31], two common methods named as P&O and INC with fuzzy control method have been compared. In [32], two MPPT methods based on fuzzy and neural control were presented and results of the methods were compared. In [33], MPPT was modelled based on INC method. In [34], PSO based MPPT technique was introduced using one pair of sensors to control PV arrays leading to lower prices, higher overall efficiency and simplicity in implementation. However, during rapidly changing conditions, these controllers do not function properly. Besides there are some other MPPT controllers based on artificial intelligence techniques such as neural networks [35], [36], intelligence algorithms [37]–[39] and fuzzy logic controllers [40]–[43] whose performance have been significantly enhanced with the help of conventional methods under variable conditions. But the main challenges associated with modelling this controller are in the type selection of fuzzy inference system, the shape and range of changes in fuzzy membership functions and fuzzy rules. In [44]–[46], heuristic methods named genetic algorithm (GA), PSO and neural networks have been introduced to optimize the parameters of FLCs; but method based on neural network has requirement of having larger data for the training purpose of the network to be within an acceptable range. Furthermore, GA can't provide a single and accurate solution for the problem because of its random nature; also requires complex and time-consuming calculations.

This paper is an extended version of [47] which proposes an advanced fuzzy controller for overcoming the above-mentioned problems. The rest of the paper is organized as follows. Section 2, Section 3 and Section 4 consists of modelling of PV array, controller's detailed modelling procedure and performance of the advance FLC (proposed) respectively which will validate the FLC's effectiveness. Section V is further devoted to analysing the performance of FLC at Teknaf, a place in Bangladesh by collecting the valid data and further calculating the irradiation and temperature level on which PV system depends as shift on those parameters will affect the PV system because it shifts the optimum power. Finally, section 6 represents conclusion.

## 2. Modelling of PV Array and Panel

A PV array is highly sensitive on irradiation and temperature level and based on this, maximum power point changes which is nonlinear in characteristics. Two kinds of characteristics associated with the cell: 1) I~V characteristic and 2) P~V characteristic. Detailed information about the equivalent circuit of a cell can be found in [48], [49].

### *2.1. Mathematical Equations for PV Array*

The equivalent circuit, calculations of the characteristics are shown below with the help of some necessary equations; besides the description of the symbols can also be found in [50]:

$$I = I_{ph} - I_d - \frac{V_d}{R_{sh}} \tag{1}$$

$$V_d = V + R_s I \tag{2}$$

$$I_d = I_o\{\exp(\frac{qV_d}{nkT}) - 1\} \tag{3}$$

By combining equations (1), (2) and (3), equation (4) can be achieved:

$$I = I_{ph} - I_o[\exp\{\frac{q}{nkT}(V + R_s I)\} - 1] - \frac{V + R_s I}{R_{sh}} \tag{4}$$

Furthermore, neglecting the two internal resistances:

$$I = I_{ph} - I_o\{\exp(AV) - 1\} \cong I_{ph} - I_o \exp(AV)\ ;\ A = \frac{q}{nkT} \tag{5}$$

The parasitic resistance with real solar cells are negligible which has been mentioned in [50]. Then the equations are proceeded into further simplification:

$$I_{sc} = I_{ph}\ (\because V = 0, I = I_{sc}) \tag{6}$$

$$I_o = I_{sc}\exp(-AV_{oc})\ (\because I = 0, V = V_{oc}) \tag{7}$$

Now the optimal operating points can be described as follows:

$$I_{pm} = I_{sc}[1 - \exp\{A(V_{pm} - V_{oc})\}] \tag{8}$$

$$A = \frac{1}{(V_{pm} - V_{oc})}\log(1 - \frac{I_{pm}}{I_{sc}}) \tag{9}$$

Here, $k_v$ and $k_i$ are $V_{pm}/V_{oc}$ and $I_{pm}/I_{sc}$ respectively and the output of the panel is 100.7 kW.

The important parameters for the array are shown in Table I.

From Equation 9, we get,

$$A = \frac{1}{(\frac{54.7}{64.2} - 1)}\log(1 - \frac{5.58}{5.96}) = 8.0788 \tag{10}$$

From Equation 8 (placing the current value), we get,

$$P = V \times I = 305.2\text{W} \tag{11}$$

The power calculated above is in Watt and it is for one module. So, the power of the of the overall PV system is 100.7 kW. The 100.7 kW PV panel uses 330 Sun Power modules consisting of 66 strings of 5 series-connected modules in parallel. As one module denoting 305.2W, the power of single cell is about 4.6 Watt. So, the accuracy of the equations is very high.

**Table I**
**Specifications for one module of the PV Array**
**Array type: Sun Power SPR-305E-WHT-D**

| Properties | Value |
|---|---|
| Number of cells in series | 96 |
| Open circuit voltage, $V_{oc}$ | 64.2 Volt |
| Short-circuit current, $I_{sc}$ | 5.96 Ampere |
| Voltage at maximum power, $V_{mp}$ | 54.7 Volt |
| Current at maximum power, $I_{mp}$ | 5.58 Ampere |
| Light generated current | 6.0092 Ampere |
| Diode saturation current | $6.3014*10^{-12}$ Ampere |
| Diode ideality factor | 0.94504 |
| Shunt resistance | 269.5934 Ohms |
| Series resistance | 0.37152 Ohms |

## 3. Proposed Fuzzy Based MPPT Controller

Owing to their heuristic nature associated with simplicity and effectiveness both for linear and nonlinear systems, fuzzy logic controllers have been widely used for industrial process in recent years [51]. Besides, fuzzy logic controllers can be made using various microcontrollers [52]–[57]. It can be found in [58] that, FLC has some advantages such as working with imprecise inputs, does not need an accurate mathematical model and can handle nonlinearity as well. FLC consists of four parts including fuzzification, inference, rule base and defuzzification [59], [60]. From [58] in table 1, FLC is considered as tracking techniques with intelligent prediction. This intelligent prediction lies in choosing the most appropriate type membership function both for input and output along with the associated range. Also from [58] in table 2, a comparison has been made among different MPPT controllers. Merging this information along with from [61] and [62] from table 1 and table 5 respectively, it can be concluded that it has high speed, high stability, no manual periodic tuning but the cost is high being a microcontroller. In spite of being costlier, it is understandable that why more concerns are given on FLC and much more research is still going on this MPPT.

As said earlier, to make it more improved and unique from other fuzzy controllers, the challenges lie in the type selection of fuzzy inference system, the shape and range of changes in fuzzy membership functions and fuzzy rules. This is an off-line controller and costs analysis are not investigated. For the design purpose, the inputs are considered as two parameters consisting voltage and power of PV array.

$$\Delta P(k) = P(k) - P(k-1)$$
$$\Delta V(k) = V(k) - V(k-1) \quad (12)$$

Where, P(k) and V(k) are the power and voltage of the PV panel at a certain instant respectively. Thus P(k-1) and V(k-1) are the power and voltage of the previous instances. At MPP of the PV panel, $\Delta P(k)$ as well as $\Delta V(k)$ are zero. The output we get from the controller is the variable duty cycle. The rule base that associates the fuzzy output to the fuzzy input is derived by inference method. The rules are based on the matter that if the previous change in voltage, $\Delta V(k)$ cause the power to rise, the variable duty cycle, $\Delta D(k)$ will be automatically tuned in such a manner that next change in voltage is in the same direction, otherwise it cause the power to drop which results to move in the opposite direction. The system is provided with necessary rules so that the stabilization occurs at a peak power point. Duty cycle is fed to the DC-DC boost converter according to the equation (13); input resistance seen from the source, $R_i$ can be matched with the load impendence, $R_L$. Thus form the maximum power transfer theorem, maximum power will be achieved.

$$R_i(k) = (1-D)^2 \times R_L \quad (13)$$

### *3.1. Fuzzification*

For both input variables, 9 membership functions cover the range of variations. For optimization process the location of these function should be optimized. Fig. 1 and Fig. 2 shows the membership functions of the input parameters which are triangular in shape.

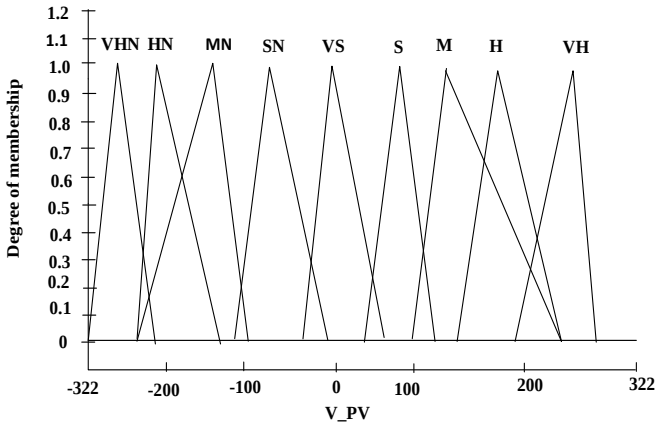


**Fig. 1.** Optimized membership function (MF) of PV panel's voltage.

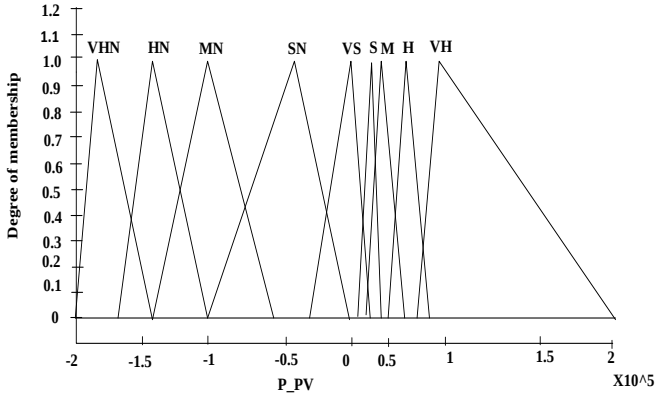


**Fig. 2.** Optimized membership function (MF) of PV panel's power.

### 3.2. *Arrangement of Fuzzy Rules*

**Table II**
**Proposed rules for fuzzy based MPPT controller**

| V_PV | | | | | P_PV |
|---|---|---|---|---|---|
| ΔD is VS | ΔD is S | ΔD is M | ΔD is H | ΔD is VH | |
| VHN<br>VS<br>MN<br>SN | | | | | VHN |
| VHN | HN<br>MN<br>SN | | | | HN |
| VHN | HN | MN<br>SN | | | MN |
| VHN | HN | MN | SN | | SN |
| VH | H | M | S | VS | VS |
| VH | VS<br>S<br>M<br>H | | | | H |
| VS<br>S<br>M<br>H<br>VH | | | | | VH |
| VH | H | M | VS<br>S | | S |
| VH | H | VS<br>S<br>M | | | M |

The most important part of modelling the controller for optimization purpose lies in the arrangement of the rules. The rules are shown in table II and Fig. 3 shows the flowchart of the controller.

Table II denotes the formulation of rules for FLC. The first row indicates: IF V_PV is VHN AND P_PV is VHN, then ΔD is VS. Similarly, for second row: IF V_PV is VS AND P_PV is VHN, then ΔD is VS.

### 3.3. *Defuzzification*

Calculation of the crisp output of the fuzzy control is done through defuzzification process and in this case, it is the variable duty cycle. Fig. 4 shows the membership function of the variable duty cycle, also triangular in shape but range covers using only five functions. The most popular methods for defuzzification are the COA (center of area), MOM (Mean of Maxima), and MCM (Max Criterion Method).

In this paper, COA is performed for the final combined fuzzy set which is denoted by the union of all rule output fuzzy sets using the maximum aggregation method [63], [64]. Consequently, the change of duty cycle is identified as follows:

$$\Delta D(k) = \frac{\sum_{j=1} \mu(\Delta D_j(k) \times \Delta D_j(k))n}{\sum_{j=1}^{n} \mu(\Delta D_j(k))} \quad (14)$$

The output of fuzzy controller is the change of duty cycle $\Delta D(k)$ which is then converted to the duty cycle following the equation:

$$D(k) = 0.55 + \Delta D(K) \quad (15)$$

For the visualization between inputs and output parameters, surface view is shown in Fig. 5.

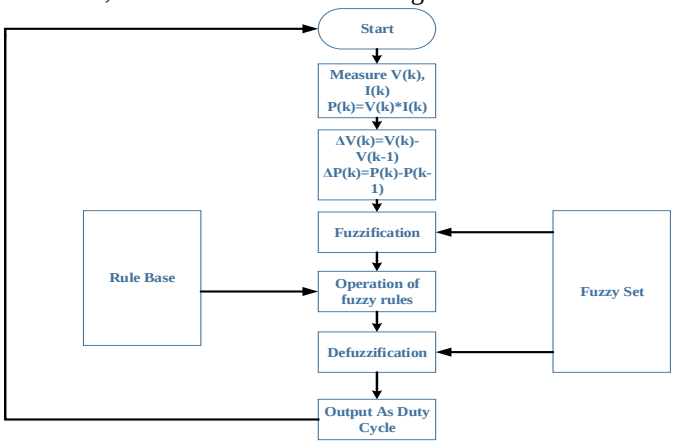


**Fig. 3.** Flow chart of the proposed controller.

### 3.4. *Optimization Technique*

At first, two parameters are considered for the input of the controller which are: PV panel's voltage and power. With the help of these parameter we are trying to find out the present operating location for panel. Another sampled voltage and power values are obtained. If increase in voltage causes power to increase, it indicates that the panel is operating on left side of the optimum point. As a result, our value of duty cycle will be according to equation 13 such that operating condition shifted towards the right side further on. But if increase in voltage causes power to decrease, it indicates that the panel is operating on right side of the optimum point. As a result, our value of duty cycle will be according to equation 13 such that operating condition shifted towards the left side further on so that operating point may reach the optimum point. After reaching the optimum point, the duty cycle tries to remain around that value unless further operating conditions (irradiation level and temperature) change.

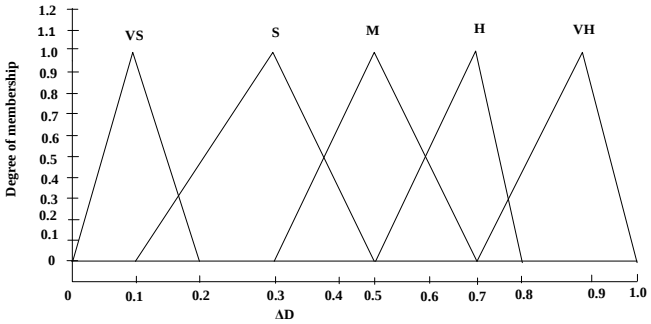


**Fig. 4.** Optimized MF of variable duty cycle.

**Fig. 5**. Surface view.

## 4. Numerical Result

### *4.1. Proposed System Model*

The proposed system is simulated using MATLAB/Simulink R2018a software. Fig. 6 shows the proposed grid connected PV system with the MPPT controller which has been operated under different conditions to ensure the effectiveness of the controller and also comparison has been made with other controllers in order to provide evidence to ensure the best performance than other compared controllers in the exact conditions described in case 1, case 2 and case 3. Here, DC-DC boost converter and 3 phase inverter with VSC controller has been used. After the conversion from DC to AC, step up transformer is used which is then finally supplied to the grid.

### *4.2. Case 1: Analysing in Variable Temperature but Constant Irradiation*

In this case, irradiation level is maintained constant at 1000 Watt/m$^2$ but temperature is varied with respect to time which is shown in Fig. 7 (a), (b).

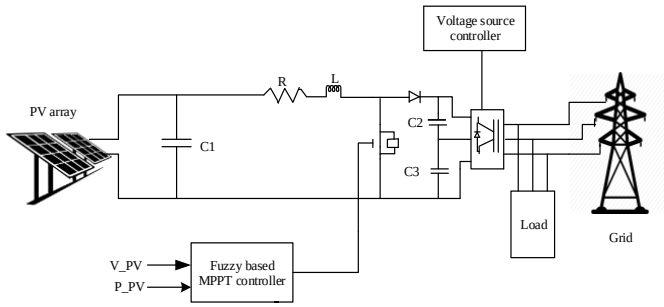


**Fig. 6.** Proposed grid connected PV system with the MPPT.

Here the proposed fuzzy logic controller has been compared with ten different controllers (six different controllers based on methodology) and for having clear indication of the effectiveness of the controllers, comparisons has been made using [47], [65]–[68] materials and also corresponding tables are shown in table III. Fig. 8 indicates the performance of the four controllers: Advance fuzzy controller is the proposed controller, incremental conductance + incremental regulator controller was given in [67], improved fuzzy controller was modelled in [47] and the controller named as P&O controller 2 was modelled in [66]. Until t=0.4 second, the PV system operates without the controller. After t=0.4 second, the system is connected with the associated MPPT controller. Extracted data from Fig. 8 can be compared to table III as considering same conditions showing better effectiveness for proposed controller.

**Table III**
**Comparison of MPPT Controllers for Case: 1**

| MPPT Controller | Output Power from the PV Panel (kW) | | |
|---|---|---|---|
| | **25** °C | **30** °C | **35** °C |
| P&O based controller 1 [65] | 90.13 | 86.73 | 83.32 |
| INC Controller [65] | 94.52 | 90.91 | 87.32 |
| GA-based optimized FLC [65] | 95.09 | 89.56 | 83.12 |
| PSO-based optimized FLC [65] | 96.03 | 90.10 | 82.56 |
| PSO-GA based optimized FLC [65] | 98.70 | 94.47 | 89.94 |
| P&O based controller 2 [66] | 95.33 | 93.93 | 92.52 |
| INC+ incremental regulator controller [67] | 95.32 | 93.93 | 92.52 |
| FLC (using I and P) [68] | 40.73 | | |
| FLC (using V and P) [68] | 80.64 | | |
| Improved FLC [47] | 81 | 66.91 | 54.45 |
| **Advanced FLC (proposed controller )** | 100.36 | 98.44 | 95.67 |

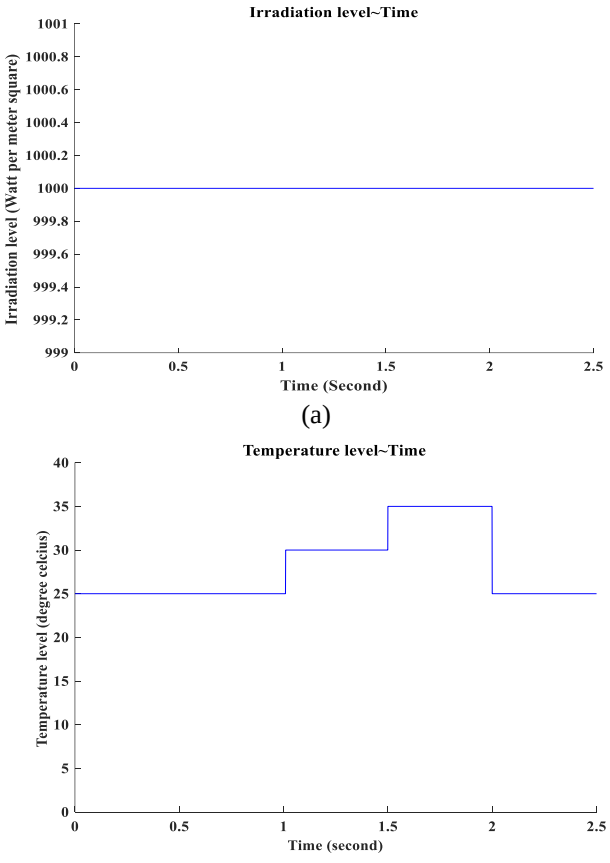


**Fig. 7.** (a) Irradiation level with respect to time (case 1). (b) Temperature level with respect to time (case 1).

**Fig. 8.** Comparison among different controllers including the proposed FLC for case 1.

**Table IV**
**Comparison of MPPT Controllers for Case: 2**

| MPPT Controller | Output Power from the PV Panel (kW) | | |
|---|---|---|---|
| | **1000 W/m$^2$** | **800 W/m$^2$** | **600 W/m$^2$** |
| P&O based controller 1 [65] | 90.13 | 71.99 | 53.68 |
| INC Controller [65] | 94.52 | 75.47 | 56.29 |
| GA-based optimized FLC [65] | 95.11 | 75.60 | 56.14 |
| PSO-based optimized FLC [65] | 96.15 | 76.32 | 56.78 |
| PSO-GA based optimized FLC [65] | 98.85 | 78.69 | 58.64 |
| P&O based controller 2 [66] | 100.4 | 80.16 | 59.86 |
| INC+ incremental regulator controller [67] | 100.4 | 80.15 | 59.85 |
| FLC (using I and P) [68] | | | |
| FLC (using V and P) [68] | | | |
| Improved FLC [47] | 90 | 71.43 | 51.74 |
| **Advanced FLC (proposed controller )** | 101.60 | 81.17 | 60.68 |

*4.3. Case 2: Analysing in Variable Irradiance but Constant Temperature*

In this event, temperature level has been kept constant but the irradiation level is varied which is shown in Fig. 9. Table IV shows the comparisons of the performances among various MPPT controllers for mentioned conditions labelled as case 2. Data extracted from Fig. 10 can be compared to table IV as proposed controller showing better effectiveness.

*4.4. Case 3: Analysing in Simultaneous Changes of Irradiance and Temperature*

In this condition, both the irradiation and temperature level are varied with respect to time according to Fig. 11 to 12. Table VI shows the comparisons of the performances among various MPPT controllers for the above case 3. Extracted data from Fig. 13 is compared to table VI as there's a clear indication that for the above cases discussed above, the proposed FLC shows best performance in tracking the magnitude of the maximum power out of the PV panel which is approximately 99%. Maximum power for 25, 30 and 35 $^{\circ}C$ are 100.7, 98.91 and 97.43 Kw respectively.

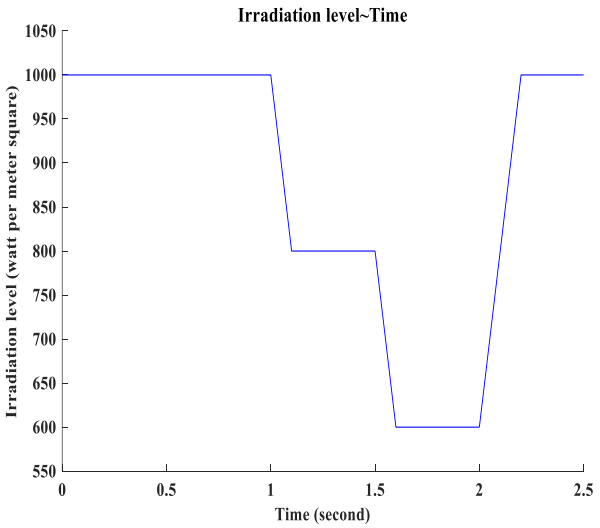


**Fig. 9:** Irradiation level with respect to time (case 2).

**Fig. 10.** Comparison among different controllers including the proposed FLC for case 2.

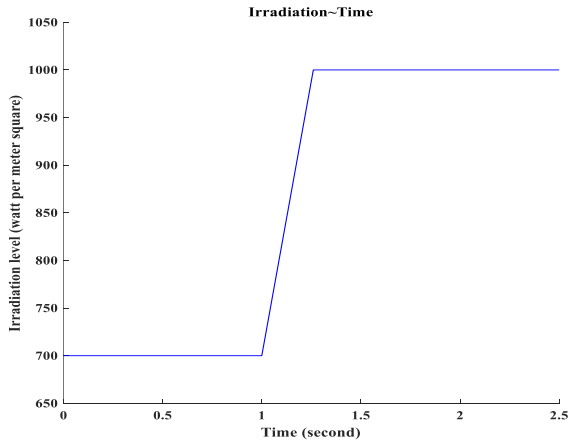


**Fig. 11.** Irradiation level (case 3).

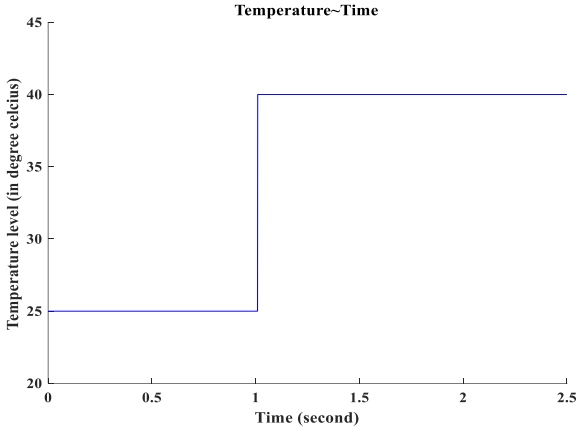


**Fig. 12.** Temperature level (case 3).

**Fig. 13.** Comparison among different controllers including the proposed FLC for case 3.

*4.5. Grid Power*

**Table V**
**Specifications of different elements**

| | | Parameters (unit) | Value |
|---|---|---|---|
| **VSC (voltage source converter)** | | Snubber resistance (ohm) | 1e^(6)=1000000 |
| | | Power electronic device | IGBT/Diodes |
| | | Internal resistance (ohm) | 0.2e^(-3)=0.0002 |
| **Three phase series RL branch** | | Resistance (ohm) | 500*e^(-6)*377/50/2=0.00754 |
| | | Inductance (H) | 500e^(-6)/2=0.00025 |
| **Three phase RLC load** | | Nominal phase to phase rms voltage (V) | 240 |
| | | Nominal frequency (Hz) | 60 |
| | | Active power (W) | 10e^(3)/100=10 |
| | | Capacitive reactive power (var) | 10e^(3)=10000 |
| **Three phase transformer (wyeg-delta)** | | Nominal power (VA) and frequency (Hz) | [100000 60] |
| | | Magnetization resistance (in per unit) | 500 |
| | | Magnetization inductance (in per unit) | 500 |
| **2 MW load (Three phase parallel RLC load)** | | Nominal phase to phase voltage (V) | 25000 |
| | | Nominal frequency (Hz) | 60 |
| | | Active power (W) | 2e^(6)=2000000 |
| **30 MW 2 Mvar load (Three phase parallel RLC load)** | | Nominal phase to phase voltage (V) | 25e^(3)=25000 |
| | | Nominal frequency (Hz) | 60 |
| | | Active power (W) | 30e^(6)=30000000 |
| | | Inductive reactive Power (var) | 2e^(6)=2000000 |
| **Three phase transformer (wyeg-delta)** | | Nominal Power (VA) and frequency (Hz) | [47e^(6) 60] |
| | | Magnetization resistance (in per unit) | 500 |
| | | Magnetization inductance (in per unit) | 500 |
| **Grounding transformer** | | Nominal Power (VA) and frequency (Hz) | [100e^(6) 60] |
| | | Nominal voltage (V) | 25e^(3)=25000 |
| | | Zero sequence resistance (per unit) and reactance (per unit) | [0.025 0.75] |
| **Three phase voltage source in series with RL branch** | **Source** | Phase to phase rms voltage (V) | 120e^(3)=120000 |
| | | Frequency (Hz) | 60 |
| | **Impedance** | 3 phase short-circuit level at base voltage (VA) | 2500e^(6)=2500000000 |
| | | Base voltage rms (V) | 120e^(3)=120000 |
| | | X/R ratio | 7 |

There are some elements connected between the grid and the PV panel for processing three phase power. After extracting the power from the panel, a 33*60 Hz, 500 V 3 level VSC (voltage source converter) has been used for converting the DC power to AC. The VSC converts the 500V DC link to 260V AC and keeps almost the unity power factor.

The three bridge arms consist of three phase RL branch and across it, connected a 10 kvar RLC load. Next a three phase wye-delta transformer is connected to the utility grid through the bus. In the utility grid, there is total (5+14) km feeder. After 5 km a 2 MW load and further (after 19 km) another 30 MW 2 Mvar load is connected. Finally a 120 kV/25 kV, 47 MVA transformer connected to a three phase voltage source in series with RL branch.

Now, atmospheric condition is considered similar to case 1 which is shown in Fig. 7. The power delivered to the grid is shown in Fig. 14. Table V contains all of the above mentioned elements information.

In each cases, the delivered power is labelled in Fig. 14. When temperature is at 25 $^{\circ}C$, the power extracted from the array is 100.36 kW, power delivered to the grid is 98.79 kW. As a result, 1.56% power loss occur from the drawing power when delivered to the grid. Similarly for 30 $^{\circ}C$ and 35 $^{\circ}C$, 1.69% and 1.81% power losses occur respectively when delivered to the grid.

For case 2, power delivered to the grid is shown in Fig. 15 and atmospheric condition in Fig. 9. As similar with the

previous one discussed above, power losses occur for 1000 watt/m$^2$, 800 watt/m$^2$ and 600 watt/m$^2$ are respectively 1.59%, 1.44% and 1.33%.

**Table VI**
**Comparison of MPPT Controllers for Case: 3**

| MPPT Controller | Output Power from the PV Array (kW) | |
|---|---|---|
| | **700 W/m$^2$, 25 ℃** | **1000 W/m$^2$, 40 ℃** |
| P&O based controller 1 [65] | 63.13 | 79.65 |
| INC Controller [65] | 65.52 | 83.24 |
| GA-based optimized FLC [65] | 66.63 | 81.79 |
| PSO-based optimized FLC [65] | 67.76 | 83.39 |
| PSO-GA based optimized FLC [65] | 69.19 | 84.91 |
| P&O based controller 2 [66] | 63.97 | 89.67 |
| INC+ incremental regulator controller [67] | 63.96 | 89.66 |
| FLC (using I and P) [68] | | |
| FLC (using V and P) [68] | | |
| Improved FLC [47] | 54.42 | 42.61 |
| **Advanced FLC (proposed controller )** | 70.02 | 91.42 |

**Fig. 14.** Power delivered to the grid for case 1.

**Fig. 15.** Power delivered to the grid for case 2.

Fig. 16-18 illustrates the percentage of power extracted from the panel by different controllers using the Table III. For each of the separate conditions the advanced FLC (proposed controller) draws the highest power comparing with the other controllers.

Similar types of figures can be formulated by using information of table IV and table VI which will ultimately indicate that in each case advanced controller performs best among other compared controllers in each separate conditions.

**Fig. 16.** Extraction of power for case 1 at 25$^0$C.

**Fig. 17.** Extraction of power for case 1 at 30$^0$C.

**Fig. 18.** Extraction of power for case 1 at $35^0$C.

*4.6. Tracking Time*

Analyzing the Fig. 8 and Fig. 10 we can found out the tracking time for each case. But from Fig. 10, we get a clear indication that when irradiation level changes from 600 to 1000 Watt/$m^2$, P&O based controller 2 lags in tracking the power according to the condition with respect to other controllers. For the tracking time, two types of events are considered: 1) power decreased due to changing conditions, 2) power increased due to changing conditions.

Fig. 8 referred to power decreasing condition; at this case the tracking time for P&O controller 2, INC+ incremental regulator controller and advanced fuzzy controller are respectively 0.025, 0.02 and 0.01 second.

Fig. 10 referred to the power increasing condition started around t=2 second; at this event the tracking time for P&O controller 2, INC+ incremental regulator controller and advanced fuzzy controller are respectively 0.284, 0.02 and 0.01 second. This time P&O controller 2 takes more time than the previous one.

*4.7. THD Analysis*

Voltage of the grid has been analyzed after filtering process which shows 0.04%THD. Table VII shows the harmonic source and Fig. 19 shows the harmonic spectrum.

**Fig. 19.** Harmonic magnitude spectrum.

**Table VII**
**Harmonic Source Data**

| Harmonic order | Magnitude (%) | Relative angle (degree) |
|---|---|---|
| 1 | 100 | -37.8 |
| 3 | 0.00 | 21.5 |
| 5 | 0.01 | 134.2 |
| 7 | 0.00 | 59.0 |
| 11 | 0.01 | 111.5 |
| 13 | 0.02 | 41.9 |
| 15 | 0.00 | 264.4 |

## 5. Performance of the FLC Considering Bangladesh's Condition, Teknaf

Geographically Bangladesh is located in South Asia, between $20^0$34' to $26^0$38' north latitude and $88^0$01' to $92^0$41' east longitude[69] . We can also acknowledge from [70] that solar energy sources in Bangladesh, 67.7%, relatively higher than other renewable energy sources (hydro, wind and others). For Bangladesh, we select Teknaf, upazila of Cox's Bazar as it is one of the highly prospective location for solar energy sources as well as the duration of the sunshine is quite constant and relatively higher (as we can see from [71] ) among others.

Table VIII shows name of the month, maximum temperature $T_{max}$, minimum temperature $T_{min}$, monthly averaged daily solar radiation $H_m$, monthly average daily hours of bright sunshine S (hour) where these data are collected from [72] and the contains associated within the brackets represents their corresponding units. With the help of these data, further the considered averaged temperature denoting the average of maximum and minimum temperature T (degree celcius) and irradiation level H (kilo Watt per meter square) are calculated. Then, the calculated temperature and

**Table VIII**

**Collection of necessary data for Teknaf, Bangladesh for further calculation of 'T' and 'H' and analyzing the performance(P_PV and P_G)**

| **Month** | **$T_{max}$** ℃ [72] | **$T_{min}$** ℃ [72] | **$H_m$** **kWh/m²** | **S** **h (hour)**[72] | **T** ℃ | **H** **W/m²** | **P_PV** **kW** | **P_G** **kW** |
|---|---|---|---|---|---|---|---|---|
| January | 30.2 | 11 | 4.73 | 8.32 | 20.6 | 568.50962 | 57.41 | 56.65 |
| February | 32.8 | 12.5 | 5.51 | 8.46 | 22.65 | 651.30024 | 65.54 | 64.75 |
| March | 34.1 | 15.4 | 6.1 | 8.54 | 24.75 | 714.28571 | 71.53 | 70.54 |
| April | 34.4 | 20.6 | 6.29 | 8.04 | 27.5 | 782.33831 | 77.69 | 76.57 |
| May | 35 | 22.3 | 5.59 | 7.02 | 28.65 | 796.2963 | 78.71 | 77.42 |
| June | 34.1 | 23.5 | 3.86 | 4.4 | 28.8 | 877.27273 | 86.77 | 85.39 |
| July | 32.9 | 23.9 | 3.16 | 2.84 | 28.4 | 1112.6761 | 110.3 | 108.4 |
| August | 33.1 | 23.8 | 3.9 | 3.2 | 28.45 | 1218.75 | 120.6 | 118.5 |
| September | 33.8 | 24.5 | 4.45 | 5.14 | 29.15 | 865.75875 | 85.49 | 84.14 |
| October | 33.8 | 22.6 | 4.6 | 6.58 | 28.2 | 699.08815 | 69.06 | 68.13 |
| November | 33.3 | 17.2 | 4.68 | 8.18 | 25.25 | 572.12714 | 56.96 | 56.2 |
| December | 30.9 | 13.7 | 4.23 | 7.68 | 22.3 | 550.78125 | 55.31 | 54.55 |

irradiation level are given as input to our PV system and observe the performance parameter of our proposed FLC: extracting of power form the PV panel, P_PV (kilo-Watt) and power fed to the grid, P_G (kilo-Watt), tracking time and THD level.

In case of analyzing the performance, similarly, two states have been considered: 1) steady state operation and 2) dynamic operation which will further validate the effectiveness of the FLC.

*5.1. Case 1: Analysing performance of FLC in Teknaf, Bangladesh considering steady state operation*

After drawing the maximum power from the PV panel, then power is fed to the grid and the amount of it is tabulated in table VIII (column 9, P_G).

**Fig. 20.** Maximum power extraction from PV panel for January by FLC.

**Fig. 21.** Maximum power extraction from PV panel for February by FLC.

**Fig. 22.** Maximum power extraction from PV panel for March by FLC.

**Fig. 23.** Maximum power extraction from PV panel for April by FLC.

**Fig. 24.** Maximum power extraction from PV panel for May by FLC.

**Fig. 25.** Maximum power extraction from PV panel for June by FLC.

**Fig. 26.** Maximum power extraction from PV panel for July by FLC.

**Fig. 27.** Maximum power extraction from PV panel for August by FLC.

**Fig. 28.** Maximum power extraction from PV panel for September by FLC.

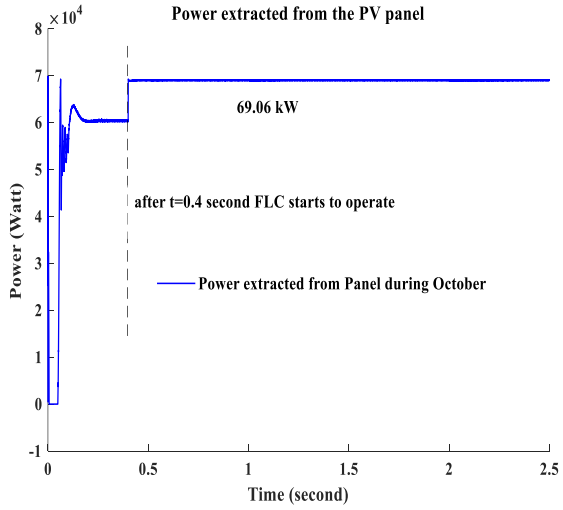


**Fig. 29.** Maximum power extraction from PV panel for October by FLC.

**Fig. 30.** Maximum power extraction from PV panel for November by FLC.

**Fig. 31.** Maximum power extraction from PV panel for December by FLC.

**Fig. 32.** Power delivered to the grid for the 6 months.

*5.2. Case 2: Analysing performance of FLC in Teknaf, Bangladesh considering dynamic state operation*

Now, consideration has given on dynamic state indicating that both irradiation level and temperature change with the passage of time.

Fig. 34 and Fig. 35 shows the irradiation and temperature level for the above mentioned 12 months respectively and again then initial condition has been restored. There have been 12 different sections numbered serially from 1 to 12 which states nothing but the months. These sections are depicted in Table IX. Fig. 36 and Fig. 37 shows power extracting from the panel and then power delivering to the grid respectively.

Through the observation, the amount of power extracted from the panel and delivered to the grid for dynamic state exactly matches with the corresponding steady state along with maintaining fast tracking i.e. requiring less time for attaining the optimal point. Thus the effectiveness of the proposed FLC is justifiable.

**Table IX**
**Illustration of the Sections**

| Number of sections | Indicated Month | Simulation starting to ending time (second) |
|---|---|---|
| 1 | January | 0 to 0.75 |
| 2 | February | 0.75 to 1 |
| 3 | March | 1 to 1.25 |
| 4 | April | 1.25 to 1.5 |
| 5 | May | 1.5 to 1.75 |
| 6 | June | 1.75 to 2 |
| 7 | July | 2 to 2.25 |
| 8 | August | 2.25 to 2.5 |
| 9 | September | 2.5 to 2.75 |
| 10 | October | 2.75 to 3 |
| 11 | November | 3 to 3.25 |
| 12 | December | 3.25 to 3.5 |
| 1 | January | 3.5 to 4 |

**Fig. 33.** Power delivered to the grid for the next six months relating Fig. 32.

**Fig. 34.** Condition of irradiation throughout the year.

**Fig. 35.** Condition of temperature throughout the year.

**Fig. 36.** Power drawing from PV panel for dynamic state.

**Fig. 37.** Power fed to the grid for dynamic state.

## 6. Conclusion

An advance fuzzy controller has been modelled for MPPT and has been compared with other controllers in several cases. In each case it shows better performance in different parameters: 1) extracting optimum power from the panel in both steady and dynamic state conditions, 2) delivering the power after extraction from panel to the grid with reduced losses, 3) very fast tracking of optimum power for the corresponding condition and 4) maintaining satisfactory level (within IEEE standard) of THD for grid voltage after completing the filtering process.

Relating the performance evaluating parameters and the cases discussed above in section 4 and 5, it is observed that the system with the proposed controller always draws up to 99% of the maximum power from the panel. It indicates very satisfactory performance in comparison to other controllers. In the proposed controller also delivers the extracted power to the grid with reduced losses which is approximately 1.5%. Also the proposed FLC is very fast in tracking optimum power as it takes only 0.01 second. Also in case of rapidly changing conditions, the FLC maintained the same tracking performance. Furthermore, grid voltage's THD level is well within the IEEE standard as showing only 0.04% after filtering which is necessary for maintaining healthy condition at the load site. Finally, some data are collected for Teknaf, Bangladesh throughout the year and performance has been evaluated which indicates the effectiveness of the proposed controller under various weather condition.

## 7. Reference

[1] N. K. Kasim, H. H. Hussain, and A. N. Abed, "Performance Analysis of Grid-Connected CIGS PV Solar System and Comparison with PVsyst Simulation Program," *Int. J. Smart Grid - ijSmartGrid*, vol. 3, no. 4, pp. 172–179, 2019.

[2] E. Demirkutlu and I. Iskender, "Grid Connected Three-Phase Boost-Inverter for Solar PV Systems," Int. J. Renew. Energy Res., vol. 11, no.2, pp. 776-784,2021.

[3] S. F. Jaber and A. M. Shakir, "Design and Simulation of a boost-Microinverter for Optimized Photovoltaic System Performance," *Int. J. Smart Grid*, vol. 5, no. 2, pp. 94–102, 2021.

[4] K. E. Okedu, H. A. L. Nadabi, and A. Aziz, "Prospects of Solar Energy in Oman : Case of Oil and Gas Industries," *Int. J. SMART GRID*, vol. 3, no. 3, pp. 138–151, 2019, [Online]. Available: https://www.ijsmartgrid.org/index.php/ijsmartgridnew/article/view/68.

[5] B. Parida, S. Iniyan, and R. Goic, "A review of solar photovoltaic technologies," *Renew. Sustain. Energy Rev.*, vol. 15, no. 3, pp. 1625–1636, 2011, doi: 10.1016/j.rser.2010.11.032.

[6] B. Zafar, "Design of a renewable hybrid photovoltaic-electrolyze-PEM/fuel cell system using hydrogen gas," *Int. J. Smart Grid-ijSmartGrid*, vol. 3, no. 4, 2019, [Online]. Available: https://ijsmartgrid.com/index.php/ijsmartgridnew/article/view/83.

[7] A. Mellit, S. A. Kalogirou, L. Hontoria, and S. Shaari, "Artificial intelligence techniques for sizing photovoltaic systems: A review," *Renew. Sustain. Energy Rev.*, vol. 13, no. 2, pp. 406–419, 2009, doi: 10.1016/j.rser.2008.01.006.

[8] A. Loukriz, M. Haddadi, and S. Messalti, "Simulation and experimental design of a new advanced variable step size Incremental Conductance MPPT algorithm for PV systems," *ISA Trans.*, vol. 62, pp. 30–38, 2016, doi: 10.1016/j.isatra.2015.08.006.

[9] S. P. Durrani, S. Balluff, L. Wurzer, and S. Krauter, "Photovoltaic yield prediction using an irradiance forecast model based on multiple neural networks," *J. Mod. Power Syst. Clean Energy*, vol. 6, no. 2, pp. 255–267, 2018, doi: 10.1007/s40565-018-0393-5.

[10] C. Ramulu, P. Sanjeevikumar, R. Karampuri, S. Jain, A. H. Ertas, and V. Fedak, "A solar PV water pumping solution using a three-level cascaded inverter connected induction motor drive," *Eng. Sci. Technol. an Int. J.*, vol. 19, no. 4, pp. 1731–1741, 2016, doi: 10.1016/j.jestch.2016.08.019.

[11] S. Messalti, A. Harrag, and A. Loukriz, "A new variable step size neural networks MPPT controller: Review, simulation and hardware implementation," *Renew. Sustain. Energy Rev.*, vol. 68, no. August 2015, pp. 221–233, 2017, doi: 10.1016/j.rser.2016.09.131.

[12] T. L. Kottas, Y. S. Boutalis, and A. D. Karlis, "New maximum power point tracker for PV arrays using fuzzy controller in close cooperation with fuzzy cognitive networks," *IEEE Trans. Energy Convers.*, vol. 21, no. 3, pp. 793–803, 2006, doi: 10.1109/TEC.2006.875430.

[13] A. Achour, D. Rekioua, A. Mohammedi, Z. Mokrani, T. Rekioua, and S. Bacha, "Application of direct torque control to a photovoltaic pumping system with sliding-mode control optimization," *Electr. Power Components Syst.*, vol. 44, no. 2, pp. 172–184, 2016, doi: 10.1080/15325008.2015.1102182.

[14] J. P. Dunlop, "Batteries and Charge Control in Stand-Alone Photovoltaic Systems Batteries and Charge Control in Stand-Alone Photovoltaic Systems Fundamentals and Application."

[15] A. N. A. Ali, M. H. Saied, M. Z. Mostafa, and T. M. Abdel- Moneim, "A survey of maximum PPT techniques of PV systems," *2012 IEEE Energytech, Energytech 2012*, 2012, doi: 10.1109/EnergyTech.2012.6304652.

[16] N. Karami, N. Moubayed, and R. Outbib, "General review and classification of different MPPT Techniques," *Renew. Sustain. Energy Rev.*, vol. 68, no. July 2015, pp. 1–18, 2017, doi: 10.1016/j.rser.2016.09.132.

[17] C. Liu, K. T. Chau, and X. Zhang, "An efficient wind-photovoltaic hybrid generation system using doubly excited permanent-magnet brushless machine," *IEEE Trans. Ind. Electron.*, vol. 57, no. 3, pp. 831–839, 2010, doi: 10.1109/TIE.2009.2022511.

[18] N. Moubayed, A. El-ali, and R. Outbib, "Control of an hybrid solar-wind system with acid battery for storage," *WSEAS Trans. POWER Syst.*, vol. 4, no. 9, pp. 307–318, 2009.

[19] M. A. Sahnoun, H. M. R. Ugalde, J. C. Carmona, and J. Gomand, "Maximum power point tracking using P&O control optimized by a neural network approach: A good compromise between accuracy and complexity," *Energy Procedia*, vol. 42, pp. 650–659, 2013, doi: 10.1016/j.egypro.2013.11.067.

[20] T. H. Kwan and X. Wu, "High performance P&O based lock-on mechanism MPPT algorithm with smooth tracking," *Sol. Energy*, vol. 155, pp. 816–828, 2017, doi: 10.1016/j.solener.2017.07.026.

[21] N. S. D'Souza, L. A. C. Lopes, and X. J. Liu, "Comparative study of variable size perturbation and observation maximum power point trackers for PV systems," *Electr. Power Syst. Res.*, vol. 80, no. 3, pp. 296–305, 2010, doi: 10.1016/j.epsr.2009.09.012.

[22] Y. Yang and H. Wen, "Adaptive perturb and observe maximum power point tracking with current predictive and decoupled power control for grid-connected photovoltaic inverters," *J. Mod. Power Syst. Clean Energy*, vol. 7, no. 2, pp. 422–432, 2019, doi: 10.1007/s40565-018-0437-x.

[23] O. Guenounou, B. Dahhou, and F. Chabour, "Adaptive fuzzy controller based MPPT for photovoltaic systems," *Energy Convers. Manag.*, vol. 78, pp. 843–850, 2014, doi: 10.1016/j.enconman.2013.07.093.

[24] Ö. Çelik and A. Teke, "A Hybrid MPPT method for grid connected photovoltaic systems under rapidly changing atmospheric conditions," *Electr. Power Syst. Res.*, vol. 152, pp. 194–210, 2017, doi: 10.1016/j.epsr.2017.07.011.

[25] S. Belhimer, M. Haddadi, and A. Mellit, "A novel hybrid boost converter with extended duty cycles range for tracking the maximum power point in photovoltaic system applications," *Int. J. Hydrogen Energy*, vol. 43, no. 14, pp. 6887–6898, 2018, doi: 10.1016/j.ijhydene.2018.02.136.

[26] A. F. Murtaza, M. Chiaberge, F. Spertino, U. T. Shami, D. Boero, and M. De Giuseppe, "MPPT technique based on improved evaluation of photovoltaic parameters for uniformly irradiated photovoltaic array," *Electr. Power Syst. Res.*, vol. 145, pp. 248–263, 2017, doi: 10.1016/j.epsr.2016.12.030.

[27] J. Ramos-Hernanz, J. M. Lopez-Guede, O. Barambones, E. Zulueta, and U. Fernandez-Gamiz, "Novel control algorithm for MPPT with Boost converters in photovoltaic systems," *Int. J. Hydrogen Energy*, vol. 42, no. 28, pp. 17831–17855, 2017, doi: 10.1016/j.ijhydene.2017.02.028.

[28] A. I. Nusaif and A. L. Mahmood, "MPPT Algorithms (PSO, FA, and MFA) for PV System Under Partial Shading Condition, Case Study: BTS in Algazalia, Baghdad," *Int. J. Smart Grid-ijSmartGrid*, vol. 4, no. 3, pp. 100–110, 2020.

[29] L. Zhang, S. S. Yu, T. Fernando, H. H. C. Iu, and K. P. Wong, "An online maximum power point capturing technique for high-efficiency power generation of solar photovoltaic systems," *J. Mod. Power Syst. Clean Energy*, vol. 7, no. 2, pp. 357–368, Mar. 2019, doi: 10.1007/s40565-018-0440-2.

[30] M. A. Elgendy, B. Zahawi, and D. J. Atkinson, "Assessment of perturb and observe MPPT algorithm implementation techniques for PV pumping applications," *IEEE Trans. Sustain. Energy*, vol. 3, no. 1, pp. 21–33, Jan. 2012, doi: 10.1109/TSTE.2011.2168245.

[31] F. Bouchafaa, I. Hamzaoui, and A. Hadjammar, "Fuzzy logic control for the tracking of maximum power point of a PV system," in *Energy Procedia*, Jan. 2011, vol. 6, pp. 633–642, doi: 10.1016/j.egypro.2011.05.073.

[32] C. Ben Salah and M. Ouali, "Comparison of fuzzy logic and neural network in maximum power point tracker for PV systems," *Electr. Power Syst. Res.*, vol. 81, no. 1, pp. 43–50, 2011, doi: 10.1016/j.epsr.2010.07.005.

[33] C. H. Lin, C. H. Huang, Y. C. Du, and J. L. Chen, "Maximum photovoltaic power tracking for the PV array using the fractional-order incremental conductance method," *Appl. Energy*, vol. 88, no. 12, pp. 4840–4847, 2011, doi: 10.1016/j.apenergy.2011.06.024.

[34] M. Miyatake, M. Veerachary, F. Toriumi, N. Fujii, and H. Ko, "Maximum power point tracking of multiple photovoltaic arrays: A PSO approach," *IEEE Trans. Aerosp. Electron. Syst.*, vol. 47, no. 1, pp. 367–380, 2011, doi: 10.1109/TAES.2011.5705681.

[35] A. B. G. Bahgat, N. H. Helwa, G. E. Ahmad, and E. T. El Shenawy, "Maximum power point traking controller

for PV systems using neural networks," *Renew. Energy*, vol. 30, no. 8, pp. 1257–1268, 2005, doi: 10.1016/j.renene.2004.09.011.

[36] R. Arulmurugan and N. Suthanthiravanitha, "Model and design of a fuzzy-based Hopfield NN tracking controller for standalone PV applications," *Electr. Power Syst. Res.*, vol. 120, pp. 184–193, 2015, doi: 10.1016/j.epsr.2014.05.007.

[37] R. Boukenoui, H. Salhi, R. Bradai, and A. Mellit, "A new intelligent MPPT method for stand-alone photovoltaic systems operating under fast transient variations of shading patterns," *Sol. Energy*, vol. 124, pp. 124–142, 2016, doi: 10.1016/j.solener.2015.11.023.

[38] Y. Mahmoud, M. Abdelwahed, and E. F. El-Saadany, "An Enhanced MPPT Method Combining Model-Based and Heuristic Techniques," *IEEE Trans. Sustain. Energy*, vol. 7, no. 2, pp. 576–585, 2016, doi: 10.1109/TSTE.2015.2504504.

[39] A. Vinayagam, A. A. Alqumsan, K. S. V. Swarna, S. Y. Khoo, and A. Stojcevski, "Intelligent control strategy in the islanded network of a solar PV microgrid," *Electr. Power Syst. Res.*, vol. 155, pp. 93–103, 2018, doi: 10.1016/j.epsr.2017.10.006.

[40] Y. T. Chen, Y. C. Jhang, and R. H. Liang, "A fuzzy-logic based auto-scaling variable step-size MPPT method for PV systems," *Sol. Energy*, vol. 126, pp. 53–63, 2016, doi: 10.1016/j.solener.2016.01.007.

[41] U. Yilmaz, A. Kircay, and S. Borekci, "PV system fuzzy logic MPPT method and PI control as a charge controller," *Renew. Sustain. Energy Rev.*, vol. 81, no. February 2017, pp. 994–1001, 2018, doi: 10.1016/j.rser.2017.08.048.

[42] A. D. Karlis, T. L. Kottas, and Y. S. Boutalis, "A novel maximum power point tracking method for PV systems using fuzzy cognitive networks (FCN)," *Electr. Power Syst. Res.*, vol. 77, no. 3–4, pp. 315–327, 2007, doi: 10.1016/j.epsr.2006.03.008.

[43] O. Z. Bakhoda, M. B. Menhaj, and G. B. Gharehpetian, "Fuzzy logic controller vs. PI controller for MPPT of three-phase grid-connected PV system considering different irradiation conditions," *J. Intell. Fuzzy Syst.*, vol. 30, no. 3, pp. 1353–1366, 2016, doi: 10.3233/IFS-152049.

[44] S. Daraban, D. Petreus, and C. Morel, "A novel MPPT (maximum power point tracking) algorithm based on a modified genetic algorithm specialized on tracking the global maximum power point in photovoltaic systems affected by partial shading," *Energy*, vol. 74, no. C, pp. 374–388, 2014, doi: 10.1016/j.energy.2014.07.001.

[45] Y. Soufi, M. Bechouat, and S. Kahla, "Fuzzy-PSO controller design for maximum power point tracking in photovoltaic system," *Int. J. Hydrogen Energy*, vol. 42, no. 13, pp. 8680–8688, 2017, doi: 10.1016/j.ijhydene.2016.07.212.

[46] R. K. Kharb, S. L. Shimi, S. Chatterji, and M. F. Ansari, "Modeling of solar PV module and maximum power point tracking using ANFIS," *Renew. Sustain. Energy Rev.*, vol. 33, pp. 602–612, 2014, doi: 10.1016/j.rser.2014.02.014.

[47] M. Naiem-Ur-Rahman, S. Newaz, and M. M. Rana, "A fuzzy based MPPT controller for PV system," in *2020 IEEE International Conference on Computing, Power and Communication Technologies, GUCON 2020*, Oct. 2020, pp. 635–638, doi: 10.1109/GUCON48875.2020.9231093.

[48] M. Zolfaghari, S. H. Hosseinian, S. H. Fathi, M. Abedi, and G. B. Gharehpetian, "A New Power Management Scheme for Parallel-Connected PV Systems in Microgrids," *IEEE Trans. Sustain. Energy*, vol. 9, no. 4, pp. 1605–1617, 2018, doi: 10.1109/TSTE.2018.2799972.

[49] A. Khalilnejad, A. Sundararajan, and A. I. Sarwat, "Optimal design of hybrid wind/photovoltaic electrolyzer for maximum hydrogen production using imperialist competitive algorithm," *J. Mod. Power Syst. Clean Energy*, vol. 6, no. 1, pp. 40–49, 2018, doi: 10.1007/s40565-017-0293-0.

[50] M. Godoy Sirnoes, "Fuzzy optimisation based control of a solar array system," *IEE Proc. Electr. Power Appl.*, vol. 146, no. 5, pp. 552–558, 1999, doi: 10. 1049/ip-epa:19990341.

[51] M. Veerachary, T. Senjyu, and K. Uezato, "Feedforward maximum power point tracking of PV systems using fuzzy controller," *IEEE Trans. Aerosp. Electron. Syst.*, vol. 38, no. 3, pp. 969–981, 2002, doi: 10.1109/TAES.2002.1039412.

[52] C. Y. Won, D. H. Kim, S. C. Kim, W. S. Kim, and H. S. Kim, "New maximum power point tracker of photovoltaic arrays using fuzzy controller," in *PESC Record - IEEE Annual Power Electronics Specialists Conference*, 1994, vol. 1, pp. 396–403, doi: 10.1109/pesc.1994.349703.

[53] M. G. Simoes, N. N. Franceschetti, and M. Friedhofer, "Fuzzy logic based photovoltaic peak power tracking controller," in *IEEE International Symposium on Industrial Electronics*, 1998, vol. 1, pp. 300–305, doi: 10.1109/isie.1998.707796.

[54] A. M. A. Mahmoud, H. M. Mashaly, S. A. Kandil, H. El Khashab, and M. N. F. Nashed, "Fuzzy logic implementation for photovoltaic maximum power tracking," in *IECON Proceedings (Industrial Electronics Conference)*, 2000, vol. 1, pp. 735–740, doi: 10.1109/IECON.2000.973240.

[55] N. Patcharaprakiti, S. Premrudeepreechacharn, and Y. Sriuthaisiriwong, "Maximum power point tracking using adaptive fuzzy logic control for grid-connected photovoltaic system," *Renew. Energy*, vol. 30, no. 11, pp. 1771–1788, Sep. 2005, doi: 10.1016/j.renene.2004.11.018.

[56] M. Veerachary, T. Senjyu, and K. Uezato, "Neural-network-based maximum-power-point tracking of coupled-inductor interleaved-boost-converter-supplied PV system using fuzzy controller," in *IEEE Transactions on Industrial Electronics*, Aug. 2003, vol. 50, no. 4, pp. 749–758, doi: 10.1109/TIE.2003.814762.

[57] N. Khaehintung, K. Pramotung, B. Tuvirat, and P. Sirisuk, "RISC-microcontroller built-in fuzzy logic controller

of maximum power point tracking for solar-powered light-flasher applications," in *IECON Proceedings (Industrial Electronics Conference)*, 2004, vol. 3, pp. 2673–2678, doi: 10.1109/IECON.2004.1432228.

[58] N. Karami, N. Moubayed, and R. Outbib, "General review and classification of different MPPT Techniques," *Renew. Sustain. Energy Rev.*, vol. 68, no. September 2016, pp. 1–18, 2017, doi: 10.1016/j.rser.2016.09.132.

[59] F. Bouchafaa, D. Beriber, and M. S. Boucherit, "Modeling and simulation of a gird connected PV generation system with MPPT fuzzy logic control," 2010, doi: 10.1109/SSD.2010.5585530.

[60] Subiyanto, A. Mohamed, and M. A. Hannan, "Maximum power point tracking in grid connected PV system using a novel fuzzy logic controller," in *SCOReD2009 - Proceedings of 2009 IEEE Student Conference on Research and Development*, 2009, pp. 349–352, doi: 10.1109/SCORED.2009.5443002.

[61] B. Bendib, H. Belmili, and F. Krim, "A survey of the most used MPPT methods: Conventional and advanced algorithms applied for photovoltaic systems," *Renew. Sustain. Energy Rev.*, vol. 45, pp. 637–648, 2015, doi: 10.1016/j.rser.2015.02.009.

[62] M. A. Eltawil and Z. Zhao, "MPPT techniques for photovoltaic applications," *Renew. Sustain. Energy Rev.*, vol. 25, pp. 793–813, 2013, doi: 10.1016/j.rser.2013.05.022.

[63] A. Messai, A. Mellit, A. Guessoum, and S. A. Kalogirou, "Maximum power point tracking using a GA optimized fuzzy logic controller and its FPGA implementation," *Sol. Energy*, vol. 85, no. 2, pp. 265–277, Feb. 2011, doi: 10.1016/j.solener.2010.12.004.

[64] E. H. Mamdani and S. Assilian, "Experiment in linguistic synthesis with a fuzzy logic controller," *Int. J. Hum. Comput. Stud.*, vol. 51, no. 2, pp. 135–147, Aug. 1999, doi: 10.1006/ijhc.1973.0303.

[65] M. Dehghani, M. Taghipour, G. B. Gharehpetian, and M. Abedi, "Optimized Fuzzy Controller for MPPT of Grid-connected PV Systems in Rapidly Changing Atmospheric Conditions," *J. Mod. Power Syst. Clean Energy*, vol. 9, no. 2, pp. 376–383, 2021, doi: 10.35833/MPCE.2019.000086.

[66] "Average Model of a 100-kW Grid-Connected PV Array - MATLAB & Simulink." https://www.mathworks.com/help/physmod/sps/ug/average-model-of-a-100-kw-grid-connected-pv-array.html?searchHighlight=Average model of a 100-kw grid-connected pv array&s_tid=srchtitle (accessed May 06, 2021).

[67] "Detailed Model of a 100-kW Grid-Connected PV Array - MATLAB & Simulink." https://www.mathworks.com/help/physmod/sps/ug/detailed-model-of-a-100-kw-grid-connected-pv-array.html;jsessionid=ebcc6cd1758ebec909f055b72aed (accessed May 06, 2021).

[68] K. H. Kapumpa and D. Chouhan, "A fuzzy logic based MPPT for 1MW standalone solar power plant," *2017 Recent Dev. Control. Autom. Power Eng. RDCAPE 2017*, vol. 3, pp. 153–159, 2018, doi: 10.1109/RDCAPE.2017.8358258.

[69] "Bangladesh - Banglapedia." https://en.banglapedia.org/index.php/Bangladesh (accessed Jul. 17, 2021).

[70] D. B. Mridul, A. K. Azad, M. K. Biswas, A. Datta, K. Mohammad, and R. Ul, "Current Scenario of Solar Energy Production in Bangladesh and Future Potentiality," no. May, 2021.

[71] S. K. Nandi, M. N. Hoque, H. R. Ghosh, and S. K. Roy, "Potential of Wind and Solar Electricity Generation in Bangladesh," *ISRN Renew. Energy*, vol. 2012, pp. 1–10, 2012, doi: 10.5402/2012/401761.

[72] "IEEE Xplore Full-Text PDF:" https://ieeexplore.ieee.org/stamp/stamp.jsp?tp=&arnumber=8975552 (accessed Jul. 18, 2021).